

Hubble Space Telescope Imaging of the Post-Starburst Quasar UN J1025–0040: Evidence for Recent Star Formation

Michael S. Brotherton¹, Matthew Grabelsky², Gabriela Canalizo³, Wil van Breugel³, Alexei V. Filippenko⁴, Scott Croom⁵, Brian Boyle⁵, Tom Shanks⁶

ABSTRACT

We present new *Hubble Space Telescope* (*HST*) WFPC2 images of the post-starburst quasar UN J1025–0040, which contains both an active galactic nucleus (AGN) and a 400-Myr-old nuclear starburst of similar bolometric luminosity ($\sim 10^{11.6} L_{\odot}$). The F450W and F814W images resolve the AGN from the starburst and show that the bulk of the star light ($\sim 6 \times 10^{10} M_{\odot}$) is contained within a central radius of about 600 parsecs, and lacks clear morphological structures at this scale. Equating the point-source light in each image with the AGN contribution, we determined the ratio of AGN-to-starburst light. This ratio is 69% in the red F814W image, consistent with our previous spectral analysis, but $\leq 50\%$ in the blue F450W image whereas we had predicted 76%. The *HST* images are consistent with previous photometry, ruling out variability (a fading AGN) as a cause for this result. We can explain the new data if there is a previously unknown young stellar population present, 40 Myr or younger, with as much as 10% of the mass of the dominant 400-Myr-old population. This younger starburst may represent the trigger for the current nuclear activity. The multiple starburst ages seen in UN J1025–0040 and its companion galaxy indicate a complex interaction and star-formation history.

¹Kitt Peak National Observatory, National Optical Astronomy Observatories, 950 North Cherry Avenue, P. O. Box 26732, Tucson, AZ 85726; mbrother@noao.edu. The National Optical Astronomy Observatories are operated by the Association of Universities for Research in Astronomy, Inc., under cooperative agreement with the National Science Foundation.

²Department of Physics and Astronomy, Rice University, Houston, TX; grabelsky@hotmail.com

³Institute of Geophysics and Planetary Physics, Lawrence Livermore National Laboratory, 7000 East Avenue, P.O. Box 808, L413, Livermore, CA 94550

⁴Department of Astronomy, 601 Campbell Hall, University of California, Berkeley, CA 94720-3411

⁵Anglo-Australian Observatory, PO Box 296, Epping, NSW 2121, Australia

⁶Department of Physics, University of Durham, South Road, Durham DH1 3LE

Subject headings: galaxies: evolution – galaxies: interactions – galaxies: starburst
– quasars: general

1. Introduction

Exciting progress has been made bolstering our understanding of the connection between active galactic nuclei (AGNs) and starbursts. It appears that essentially every large galaxy harbors a supermassive dark object (presumably a black hole) some 0.15% of the mass of its spheroidal component (Magorrian et al. 1998; Gebhardt et al. 2000a), although the black hole mass perhaps correlates more tightly with the velocity dispersion of the host bulge (e.g., Gebhardt et al. 2000b; Ferrarese & Merritt 2000a). These are plausibly “dead” quasars, which once burned while undergoing high accretion episodes. Furthermore, black hole masses for “live” quasars determined from reverberation techniques also correlate with the bulge mass and velocity dispersion (Gebhardt et al. 2000b; Ferrarese et al. 2001). Consistent with these results, there exists an upper limit to the luminosity of AGNs that depends on their host galaxy stellar mass (e.g., McLeod, Rieke, & Storrie-Lombardi 1999). Finally, there is the global similarity in the strong evolution of the quasar luminosity function and the star-formation rate (e.g., Boyle & Terlevich 1998).

These points have sparked much recent theoretical interest in hierarchical galaxy formation and related scenarios featuring direct relationships between star formation and the growth/fueling of central black holes (e.g., Burket & Silk 2001, and references therein). AGN activity, in fact, may reflect a fundamental stage of galaxy evolution.

The discovery of a large population of ultraluminous infrared galaxies (ULIRGs; $L_{IR} > 10^{12}L_{\odot}$) that are strongly interacting merger systems heated by both starburst and AGN power sources led Sanders et al. (1988) to hypothesize that ULIRGs represent the initial dust-enshrouded stage of a quasar (see also Sanders & Mirabel 1996 for a review). The evidence for this evolutionary scenario is circumstantial, but the hypothesis is supported by *HST* images of warm ULIRGs and optical QSOs that show similarities such as knots of recent star formation (e.g., Surace et al. 1998; Boyce et al. 1996; Bahcall et al. 1997). But Boyce et al. (1996) suggested that the *IRAS*-selected quasars are the products of *young* spiral mergers, not old mergers. Recent *ISO* results may also be incompatible with a strict evolutionary scenario: Genzel et al. (1998) surveyed ULIRGs and found that half contain simultaneously an AGN and starburst activity in a 1-2 kpc circumnuclear ring (these very young star-forming regions have ages 10-100 Myrs), but that the presence of an AGN is *not*

correlated with the merger age (see also Canalizo & Stockton 2001).

During the course of identifying quasar candidates in the AAT-2dF quasar survey (Croom et al. 2001) coincident with radio sources in the NRAO VLA Sky Survey (NVSS; Condon et al. 1998), we discovered UN J1025–0040 (Brotherton et al. 1999a). This object’s unusual spectrum shows the broad Mg II emission line of a quasar as well as the large Balmer jump and deep Balmer absorption lines reminiscent of an A-type star, all at $z = 0.634$. The spectrum may be categorized as a “Q + A” (quasar plus post-starburst) spectrum similar to those of post-starburst galaxies which have “k + A” spectra due to the combination of young and old stellar populations. We modeled the stellar content of UN J1025–0040 using stellar synthesis population models (Bruzual & Charlot 1996), and found that a 400-Myr-old instantaneous starburst provides an excellent match to the Balmer jump and stellar absorption lines. In conjunction with the broad emission lines and power-law spectrum of a blue quasar, the observed spectrum could be completely accounted for, although not uniquely. A population of very young stars could also be present, but such a population lacks strong features in the observed spectral region to betray its presence (ultraviolet spectroscopy or imaging analysis, as in this paper, is needed).

The estimate of the initial mass of the 400-Myr-old starburst was nearly $10^{11} M_{\odot}$, or the mass of our own Milky Way Galaxy. Subtracting off this model left a residual spectrum that resembles a normal if rather excessively blue quasar. The total energy budget of both components appeared similar, $10^{11.6} L_{\odot}$. Running the stellar synthesis population model in reverse, when the starburst was only 50 Myr old it would have had a bolometric luminosity of $10^{12.4} L_{\odot}$ and qualified as an ULIRG.

Deep Keck K_s -band imaging with $0.5''$ seeing failed to resolve quasar and stellar components although it did reveal a companion galaxy $4.2''$ away that turned out to have a dominant 800-Myr-old stellar population (Canalizo et al. 2000). Faint [O II] $\lambda 3727$ knots are also present between UN J1025–0040 and the companion. Certainly this is an interacting system, as are essentially all ULIRGs.

With these results in hand, we were awarded *HST* cycle 9 time to image UN J1025–0040 with WFPC2 and attempt to resolve the starburst from the quasar. The sub-pixel dithered resolution of the WFPC2 PC achieves a spatial resolution of about 600 parsecs FWHM at $z = 0.634$ ($H_0 = 75 \text{ km s}^{-1} \text{ Mpc}^{-1}$, $q_0 = 0$), and we anticipated seeing a $\sim \text{kpc}$ -scale starburst ring or a double nucleus.

We do not resolve any such structures (§ 2). We marginally resolve extended emission (stars) around a point source (the AGN) and see a disturbed morphology suggestive of a nuclear merger remnant (§ 3). The ratio of the point-to-extended light differs from the

spectral analysis of Brotherton et al. (1999a) and indicates the presence of a previously unsuspected young or on-going starburst (§ 4). We discuss the implications of these results (§ 6) and summarize our conclusions (§ 7).

2. *HST* Images

We imaged UN J1025–0040 in two broad bands, F814W in the red longward of the redshifted Balmer jump, and F450W in the blue shortward of the redshifted Balmer jump. UN J1025–0040 was centered on the Planetary Camera (PC) detector of WFPC2 (0.046 arcsec per pixel), and multiple images at each band were taken using a sub-pixel dithered box pattern for maximum resolution. Eight 500 sec observations were made on 13 Apr 2001 (UT) through the F814W filter, and sixteen 500 sec observations on 20 Apr 2001 (UT) through the F450W filter.

We began with the pipeline-calibrated images which already had undergone bias subtraction and flat fielding. We combined our dithered images using two different methods, the DRIZZLE algorithm of Fruchter et al. (1997), and the algorithm of Lauer (1999). Both algorithms produce images with twice the original number of pixels along each axis, 0.023 arcsec per pixel in the case of the PC. These combination procedures also efficiently clean cosmic rays. An examination of the profiles of the resulting images showed that the algorithm of Lauer (1999) produced sharper images. For the blue F450W images, the FWHMs of cross-cuts through the point-source-dominated peaks were 3.165 pixels versus 3.875 pixels, and for the red F814W image the FWHMs were 4.537 and 5.042 pixels, respectively, with the Lauer reduction superior in each case. We therefore used the images produced by the Lauer (1999) algorithm for our analyses, which are shown in Figures 1 and 2.

The compact companion galaxy 4.2" to the south-southwest is detected and resolved for the the first time in these *HST* images. In the F450W image the companion spans a total spatial extent of 0.23" and in the F814W image 0.35"; the size in the red image is then 2 kpc for $h = 0.75$, which was approximately the limit reported by Canalizo et al. (2000). Table 1 gives the photometry of the integrated flux of UN J1025–0040 and its companion through the F450W and F814W filters. Figure 3 shows that the photometry is in good agreement with that reported by Canalizo et al. (2000), indicating that the AGN has not varied significantly between the two epochs. This point will be important in reaching some of our conclusions below. The magnitudes of the companion galaxy are also entirely consistent with our previous ground-based photometry.

3. Image Analysis

From the fully reduced images it is apparent that we have failed to clearly resolve any significant starburst structures (e.g., a second nucleus or a ring). The images do resolve much of the centrally concentrated starburst, which is extended over a diameter of ~ 1 kiloparsec around the sharper point source nucleus that is the AGN. Some spurs of low surface brightness extended outward, the most notable being toward the northeast. A low surface brightness plateau extends to the west about 0.5 arcsec. The outermost surface brightness contour in the red image shows is perhaps suggestive of a merger.

There were no suitable stars in the image field of the PC, so we used the Tiny Tim software (Krist & Hook 1999) to produce model PSFs in conjunction with the spectral shape of the point source, a blue quasar, in this case using a composite quasar spectrum (Brotherton et al. 2001). We tried different values of the jitter parameter to find the best estimate for the PSF in each image, as telescope breathing and detector effects make the PSF impossible to model perfectly. The jitter added was 14 mas for the F450W model, and 18 mas for the F814W model.

Once we had good estimates of the PSFs, we used the Richard-Lucy algorithm to deconvolve our images. These deconvolved images did not reveal any significant additional detail. We have a disturbed nuclear region with a centrally concentrated, amorphous structure marginally resolved at the PC scale. The very low level extended (arcsecond scale) starlight is energetically negligible compared to the centrally concentrated light. This surrounding “fuzz” has colors that are very red, $m(F450W) - m(F814W) = 2.0$ mag in the northeast and $m(F450W) - m(F814W) = 1.6$ mag in the west, indicating an old (1+ Gyr) stellar population.

We also created PSF-subtracted images to determine the ratio of point source to extended flux. The minimum amount of point source present was estimated by subtracting off increasing amounts of the PSF model until a smooth residual was obtained that did not have a central dip. The maximum amount was estimated by subtracting off increasing amounts of the PSF model until zero flux was reached in the residual. This uncertainty dominates those present in the choice of PSF model. We estimate that the extended emission represents $52 \pm 4\%$ of the total flux in the F450W image, and $69^{+40}_{-5}\%$ in the F814W image.

4. Spectral Analyses: Quasar and Starbursts

Figure 4 shows an adaptation of a figure from Brotherton et al. (1999a), in which a 400-Myr-old instantaneous starburst accounts for the stellar light in UN J1025–0040 and

a rather blue AGN accounts for the remainder. This previous analysis indicated that the starburst contributes some two-thirds of the red light, and one quarter to one third of the blue light. The size of the Balmer jump and the depths and equivalent width ratios of the stellar absorption lines provided excellent constraints in the red part of the spectrum, but there are few stellar features in the blue to check the model.

The image analysis described in the previous section provides an independent estimate of the fractions of AGN and starburst in each band. While there is good agreement in the red F814W band between the starburst fractions determined by the image analysis and the previous spectral analysis, the blue F450W band shows a surprise. The starburst fraction in the blue is *half* the total, not $\sim 30\%$ as expected, a significant difference.

We have an excess of extended blue light, so it cannot arise from direct AGN light. The polarization is low (1-2%; Brotherton et al. 1999a) so it cannot arise from indirect, scattered light from the AGN, and the size of the scattering region would have to be implausibly large.

Single-age starbursts cannot simultaneously explain the spectral features in the red part of the spectrum and the blue-red spectral energy distribution, even when allowing the several free parameters to vary (e.g., metallicity, dust, initial mass function).

Very young stars can contribute significant blue light, while at the same time having only weak Balmer jumps and weak absorption lines. Such a population, added to a 400-Myr-old population, can make a composite starburst spectrum bluer yet allow it to retain essentially the same Balmer jump and absorption line equivalent width ratios (which are unaffected by the diluting quasar light). Figure 5 illustrates again the spectrum of UN J1025–0040 as in Figure 4, but also shows the total light photometry, the estimated starburst photometry, and a composite starburst population model. The composite model was created using Bruzual & Charlot (1996) stellar synthesis population models with two instantaneous starbursts (Salpeter IMF, solar metallicity, no dust), one 400 Myr old, the other 40 Myr old or younger (10 Myr old in the case of Fig. 5), scaled to match the combination of imaging and spectral constraints. Young starbursts older than 40 Myr are increasingly red, have larger Balmer jumps, and more pronounced absorption lines; such populations are still bluer than the 400 Myr old model and capable of meeting the imaging constraints when added in the correct proportions, but will fail to simultaneously match the spectral constraints of the Balmer jump and absorption lines.

As discussed previously by Brotherton et al. (1999a), varying the model parameters (primarily metallicity) can result in somewhat different ages. In the face of increasing complexity of this system and the limited data so far available, determining the exact parameters and ages is not yet possible. Nevertheless, we have a robust result that a significantly younger

stellar population is present in the nucleus of UN J1025–0040.

The residual quasar spectrum implied by this analysis is not as blue as originally suggested by Brotherton et al. (1999a). The quasar continuum can be approximated by a power-law continuum where the optical spectral index $\alpha = -0.5$, where $f_\nu \propto \nu^\alpha$. This is a very typical optical power-law index (e.g., Francis 1993).

How young (and hence also how massive) is the young starburst? How does its presence affect our previous conclusions regarding the older, more massive starburst? Figure 6 shows a range of viable models. All models shown are combinations of dust-free instantaneous starbursts employing Salpeter initial mass functions and solar metallicities, and the composite quasar spectrum of Brotherton et al. (2001) based on the FIRST Bright Quasar Survey (FBQS; White et al. 2001). The combination of bright optical selection and deep radio selection in the FBQS is rather similar to that used for the 2dF-NVSS selection that identified UN J1025–0040. This composite quasar spectrum has a power-law index of $\alpha = -0.46$, consistent with that determined above.

The scaling, and hence mass, of the 400-Myr-old starburst is rather insensitive to the age of the younger population. For the updated photometry here and for $H_0 = 75 \text{ km s}^{-1} \text{ Mpc}^{-1}$, $q_0 = 0$, the oldest composite starburst model of Figure 6 contains a 400-Myr-old starburst with $5.7 \times 10^{10} M_\odot$, plus a 40-Myr-old starburst with $6.7 \times 10^9 M_\odot$, or 10% of the mass of the older starburst. For the youngest models of Figure 6 (0 and 1.5-Myr-old instantaneous bursts), the starburst masses are down another order of magnitude, or about 1% of the mass of the older starburst. At a good fraction of $10^9 M_\odot$, this still qualifies as a very massive starburst in its own right. The exact parameters are not well determined and require additional constraints in the form of ultraviolet spectroscopy. The caveats of Brotherton et al. (1999a) regarding the uncertainties on the age and mass of the older starburst should also be kept in mind.

5. Discussion

The primary aim of obtaining the *HST* images was to resolve the starburst from the AGN and identify any morphological structures that might provide a guide as to the origin of such an extremely massive starburst. In that, we have been partially successful, insofar as we can distinguish a point source from a more diffuse region of centrally concentrated starlight. Since the ratio of starlight to quasar in the red part of spectrum is just as predicted from the spectral analysis of Brotherton et al. (1999a), we are probably not missing any core of starlight still unresolved from the AGN.

We were not successful in identifying any clearly recognizable star-forming structures, such as a starburst ring as has been seen in some other AGNs (e.g., NGC 985, Rodriguez Espinosa & Stanga 1990). At these redshifts the *HST* resolution is only probing the marginally sub-kiloparsec scale, so it is still possible that such an organized structure exists on smaller scales but is not yet resolvable as such.

These shallow images do not reveal as much detail outside the nucleus as do the deeper low-resolution ground-based images (Brotherton et al. 1999a; Canalizo et al. 2000). The nuclear structure is revealed to be non-uniform and suggestive of an evolved merger product, perhaps similar to Arp 220 (e.g., Scoville et al. 1998), but not as dusty. Whether or not UN J1025–0040 is an actual merger product or merely disturbed and interacting will likely require much deeper high-spatial-resolution images. Interpreting UN J1025–0040 as a merger product, however, would be entirely consistent with the evolutionary hypothesis of Sanders et al. (1988) in which the end result of massive mergers would be such a post-starburst quasar. This evolutionary hypothesis has been recently boosted by detailed work on the IRAS 1-Jy sample of ULIRGs (e.g., Veilleux, Kim, & Sanders 1999) which shows an increasing fraction of luminous AGNs with increasing merger age. This is a large, complete sample that includes primarily the most luminous ULIRGs for which the evolutionary hypothesis may hold true overall; contrary results, like those of Genzel et al. (1998), may result from small samples including less luminous ULIRGs. This is an ongoing area of debate.

The new result of the presence of a young (≤ 40 Myr) starburst adds to this debate, indicating that specific systems can indeed be complex. Canalizo & Stockton (1997) suggested that in an evolutionary progression, the age of a starburst is a clock indicating the age of the AGN activity (Canalizo & Stockton 2001 strengthens the original arguments but also provides additional caveats). This assumes that the fueling of the nuclear starburst and the central black hole occurs at the same time, and that the black hole continues to be fueled. Determining the ages of starbursts in AGN systems would then permit the quasar lifetime to be estimated, and the quasar duty cycle as well. These numbers would complement those determined from combining the evolution of the quasar luminosity function and the population of relic black holes today in the local universe. The complication of our new result is that there has been a substantial starburst in UN J1025–0040 much more recently than 400 Myr, and this starburst may represent the appropriate clock for the current activity. The AGN may well not shine steadily, but undergo bursts that correspond to events that provide fuel and also incite star formation.

Our measurements of the starburst masses in the nucleus of UN J1025–0040, a total of $6\text{--}7 \times 10^{10} M_{\odot}$, represent an estimate or at least lower limit to the host galaxy bulge mass. We can estimate the AGN properties, black hole mass and fraction of the Eddington

luminosity at which it shines, using techniques alluded to in the introduction (following the formalism and choice of parameters of Merritt & Ferrarese 2001, which includes our chosen cosmology). A black hole mass is estimated by assuming Keplerian motions of ionized gas in a spherical broad emission line region (BLR), with a velocity $v_{BLR} = \sqrt{3}/2 \text{ FWHM}(H\beta)$ at a distance $R_{BLR} = 32.9(\lambda L_{5100}/10^{44} \text{ ergs s}^{-1})^{0.7}$ light days (Kaspi et al. 2000). The FWHM of the $H\beta$ line is rather uncertain given the contamination from the strong stellar spectrum. The FWHM of Mg II is generally consistent with that of $H\beta$, certainly so within the uncertainty of this sort of black hole estimate, so we adopt $\text{FWHM}(H\beta) = 5500 \text{ km s}^{-1}$ (Brotherton et al. 1999a). This yields $M_{BH} = 2.7 \times 10^8 M_{\odot}$, and $M_{BH}/M_{Bulge} = 0.04\%$, which is within the sample range of local AGN but smaller than the average $\langle M_{BH}/M_{bulge} \rangle \sim 0.1\%$ (Merritt & Ferrarese 2001). We estimate the bolometric luminosity as $L_{bol} = 9\lambda L_{\lambda}$, where λL_{λ} is evaluated at 5500 \AA (Kaspi et al. 2000), obtaining $5.7 \times 10^{11} L_{\odot}$, consistent with our previous value (Brotherton et al. 1999a). For our black hole mass estimate, the Eddington luminosity is $1.0 \times 10^{13} L_{\odot}$, and the Eddington fraction $L/L_{Edd} = 0.05$. These values are all consistent with those of other QSOs and Seyfert galaxies so far studied, so nothing stands out as particularly extreme other than the starburst.

While the extremely massive starburst of UN J1025–0040 might suggest that it is an isolated case of limited applicability, it actually represents the prototype of an entire *class* of post-starburst QSOs. The 2dF QSO Redshift Survey now contains close to 23000 QSOs at $z < 3$ and $B < 21$ (e.g., Croom et al. 2001). Some $\sim 3\%$ of $z < 0.75$ quasars (94/2939) show evidence of Balmer jumps and high-order Balmer absorption lines at the 3σ level (Croom et al. in prep.). Determining the starburst ages and masses in conjunction with the AGN properties (e.g., black hole mass, Eddington fraction as above) for a large sample may lead to a consistent picture for the relationship between AGNs and the evolution of the galaxies that host them, something that we cannot yet do given only the singular case of UN J1025–0040. For instance, we might expect to find that the starburst age correlates with M_{BH}/M_{bulge} since older quasars will have had more time to accrete the available fuel, and inversely correlates with L/L_{Edd} since that fuel must eventually be exhausted.

Quantitatively developing the evolutionary scenario will probably still be insufficient to explain all vectors leading to nuclear activity and their duty cycles. Besides the 97% of 2dF QSOs that do not show clear spectroscopic evidence for (extremely) massive starbursts and which may not represent evolved ULIRGs, there are binary quasars. There are around a dozen binary quasars currently known, and the indications are that the nuclei are triggered *early* in a galactic merger process by tidal forces when the galaxies are some 50-100 kpc apart (Mortlock et al. 1999). The post-starburst quasar that is FIRST J1643+3156B, the fainter member of a binary quasar system (Brotherton et al. 1999b), would fit right into the post-starburst quasar sample of the 2dF. High-quality follow-up imaging of that sample may

reveal binary quasars like FIRST J1643+3156 in addition to evolved starburst mergers like UN J1025–0040. Starburst age would therefore appear to be a superior clock of fuel flow compared to merger age, in characterizing nuclear activity, and should be measured when possible.

Only a decade ago, debate focused upon whether the majority of quasars had “fuzz” around them or not. *HST* and ground-based near-IR imaging then opened up the study of quasar host galaxies in general. Today we are starting to characterize their stellar populations and may be on the verge of reconstructing their evolutionary histories. In the future, studies of the evolution of galaxies and AGN may be impossible to separate.

6. Summary

High-resolution images using WFPC2 on the Hubble Space Telescope show that UN J1025–0040 has a disturbed, compact nucleus, but no easily identifiable morphological structures. The photometry is consistent with that of Canalizo et al. (2000) indicating the AGN has not varied significantly between the time the ground-based data was taken and the *HST* images. The F450W and F814W images can be decomposed into a point source (the AGN) and residual, somewhat extended emission (starlight) concentrated within the central several hundred parsecs. The ratio of AGN to starlight in the red F814W image is consistent with the previous spectral analysis of Brotherton et al. (1999a), but the ratio in the blue F450W image is much smaller than expected, indicating the presence of a young stellar population. The currently available data constrain the young stars to be anywhere from a ~ 40 -Myr-old population with 10% of the mass of the dominant 400 Myr starburst, to a currently active starburst having 1% of the mass – these would still constitute massive starbursts in their own right. The older starburst dominates the light at red wavelengths, and the young starburst dominates the light at UV wavelengths. This young starburst may represent the trigger of the current AGN activity.

We thank Tod Lauer for providing his image-reduction software. Matthew Grabelsky acknowledges support from the NOAO/KPNO Research Experiences for Undergraduates program funded by the National Science Foundation. Support for proposal GO-08703 was provided by NASA through a grant from the Space Telescope Science Institute, which is operated by the Association of Universities for Research in Astronomy, Inc., under NASA contract NAS 5-26555. A.V.F. acknowledges the Guggenheim Foundation for a Fellowship. A portion of this work has been performed under the auspices of the U.S. Department of Energy, National Nuclear Security Administration by the University of California, Lawrence

Livermore National Laboratory under Contract W-7405-ENG-48.

REFERENCES

- Bahcall, J. N., Kirhakos, S., Saxe, D. H., & Schneider, D. P. 1997, *ApJ*, 479, 642
- Becker, R. H., White, R. L., & Helfand, D. J. 1995, *ApJ*, 450, 559
- Boyce, P. J., et al. 1996, *ApJ*, 473, 760
- Boyle, B. J., & Terlevich, R. J. 1998, *MNRAS*, 293, L49
- Brotherton, M. S. et al. 1999a, *ApJ*, 520, L87
- Brotherton, M. S., Gregg, M. D., Becker, R. H., Laurent-Muehleisen, S. A., White, R. L., & Stanford, S. A. 1999b, *ApJ*, 514, L61
- Brotherton, M. S., Tran, H. D., Becker, R. H., Gregg, M. D., Laurent-Muehleisen, S. A., & White, R. L. 2001, *ApJ*, 546, 775
- Bruzual, A. G., & Charlot, S. 1996, unpublished
- Burkert, A. & Silk, J. 2001, *ApJL*, 554, L151
- Canalizo, G., Stockton, A., Brotherton, M. S., & van Breugel, W. 2000, *AJ*, 119, 59
- Canalizo, G. & Stockton, A. 1997, *ApJ*, 480, L5
- Canalizo, G. & Stockton, A. 2001, *ApJ*, 555, 719
- Condon, J., Cotton, W. D., Greissen, E. W., Yin, Q. F., Perley, R. A., Taylor, G. B., & Broderick, J. J. 1998, *AJ*, 115, 1693
- Croom, S. M., et al. 2001, *MNRAS*, 322, L29
- Ferrarese, L. & Merritt, D. 2000, *ApJL*, 539, L9
- Ferrarese, L., Pogge, R., Peterson, B., Merritt, D., Wandel, A., & Joseph, C. 2001, *ApJL*, 555, L79
- Francis, P. J. 1993, *ApJ*, 407, 519

- Fruchter, A. S., Hook, R. N., Busko, I. C., & Mutchier, M. 1997, The 1997 *HST* Calibration Workshop with a New Generation of Instruments, ed. by Stefano Casertano, et al. (Baltimore, MD : Space Telescope Science Institute), 518
- Gebhardt, K., et al. 2000a, *ApJL*, 543, L5
- Gebhardt, K., et al. 2000b, *ApJL*, 539, L13
- Genzel, R., et al. 1998, *ApJ*, 498, 579
- Kaspi, S., Smith, P. S., Netzer, H., Maoz, D., Jannuzi, B. T., & Giveon, U. 2000, *ApJ*, 533, 631
- Krist, J., & Hook, R. 1999, Tiny Tim User’s Guide (Version 5.0, 1999 November) (Baltimore: STScI)
- Lauer, T. R. 1999, *PASP*, 111, 227
- Magorrian, J., et al. 1998, *AJ*, 115, 2285
- McLeod, K. K., Rieke, G. H., & Storrie-Lombardi, L. J. 1999, *ApJ*, 511, L67
- Merritt, D., & Ferrarese, L. 2001, *ASP Conf. Ser.:* The Central kpc of Starbursts and AGN, astro-ph/0107134
- Mortlock, D. J., Webster, R. L., & Francis, P. J. 1999, *MNRAS*, 309, 836
- Rodriguez Espinosa, J. M. & Stanga, R. M. 1990, *ApJ*, 365, 502
- Sanders, D. B. & Mirabel, I. F. 1996, *ARA&A*, 34, 749
- Sanders, D. B., Soifer, B. T., Elias, J. H., Neugebauer, G., & Matthews, K. 1988, *ApJ*, 328, L35
- Scoville, N. Z., et al. 1998, *ApJ*, 492, L107
- Stockton, A. & Ridgway, S. E. 1991, *AJ*, 102, 488
- Surace, J. A., Sanders, D. B., Vacca, W. D., Veilleux, S., & Mazzarella, J. M. 1998, *ApJ*, 492, 116
- Veilleux, S., Kim, D.-C., & Sanders, D. B. 1999, *ApJ*, 522, 113

Table 1. Photometry^a

Object	F450W (mag)	F814W (mag)
UN J1025–0040	19.04	19.58
Companion	25.05	24.38

^aMagnitude zeropoints are used such that Vega’s spectrum integrated over the bandpass is exactly magnitude zero.

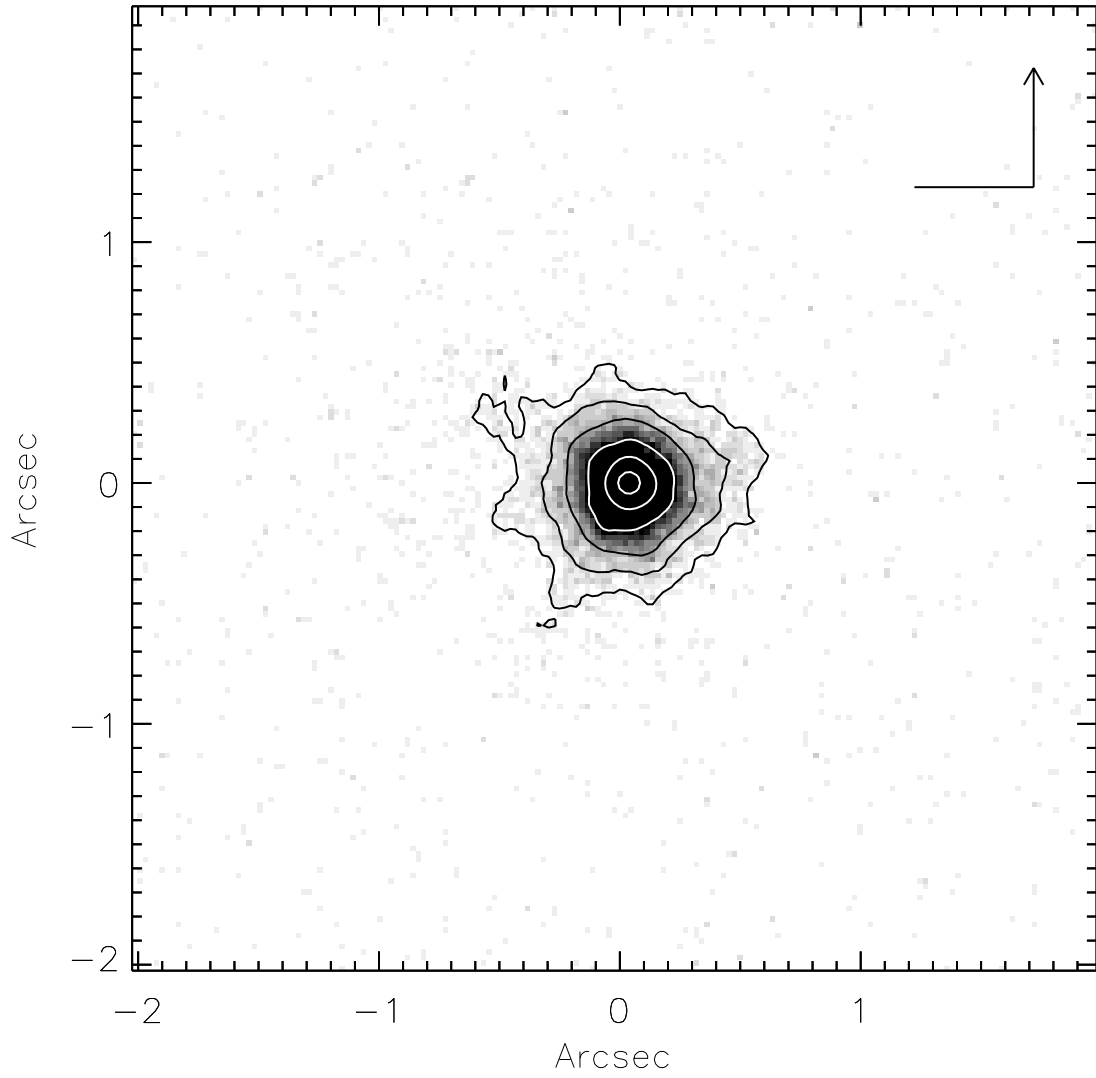


Fig. 1.— *HST* image of UN J1025–0040, F450W filter on the PC of WFPC2, using the reduction of Lauer (1999). The outer contour corresponds to 21.7 mag per arcsecond², the inner 15.5 mag per arcsecond². North (arrow) and east are indicated. The scale is $4.3 h^{-1}$ kpc/arcsec ($q_o = 0$).

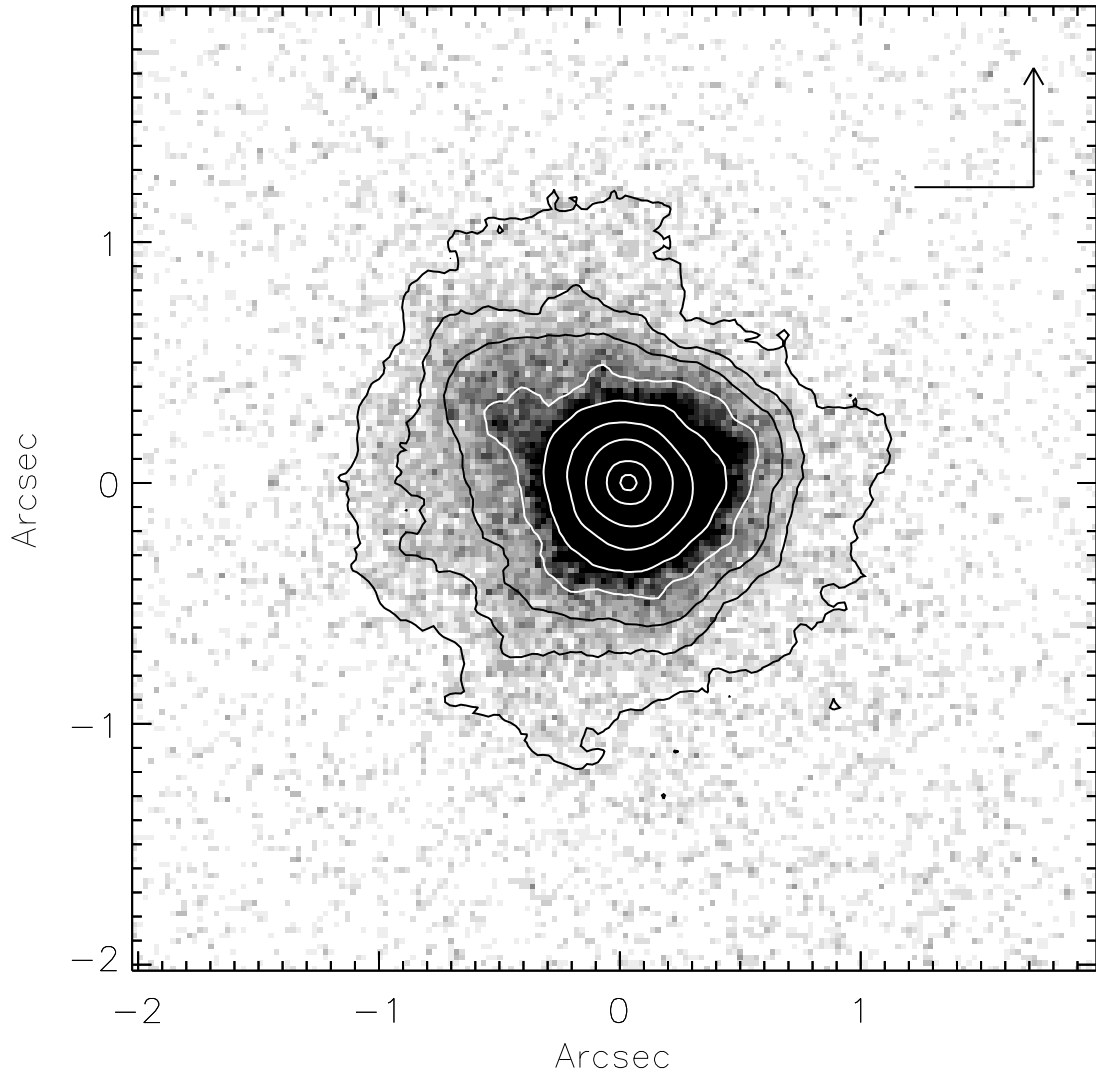


Fig. 2.— *HST* image of UN J1025–0040, F814W filter on the PC of WFPC2, using the reduction of Lauer (1999). The outer contour level corresponds to 23.4 mag per arcsecond², the inner 16.8 mag per arcsecond². North (arrow) and east are indicated. The scale is $4.3 h^{-1}$ kpc/arcsec ($q_o = 0$).

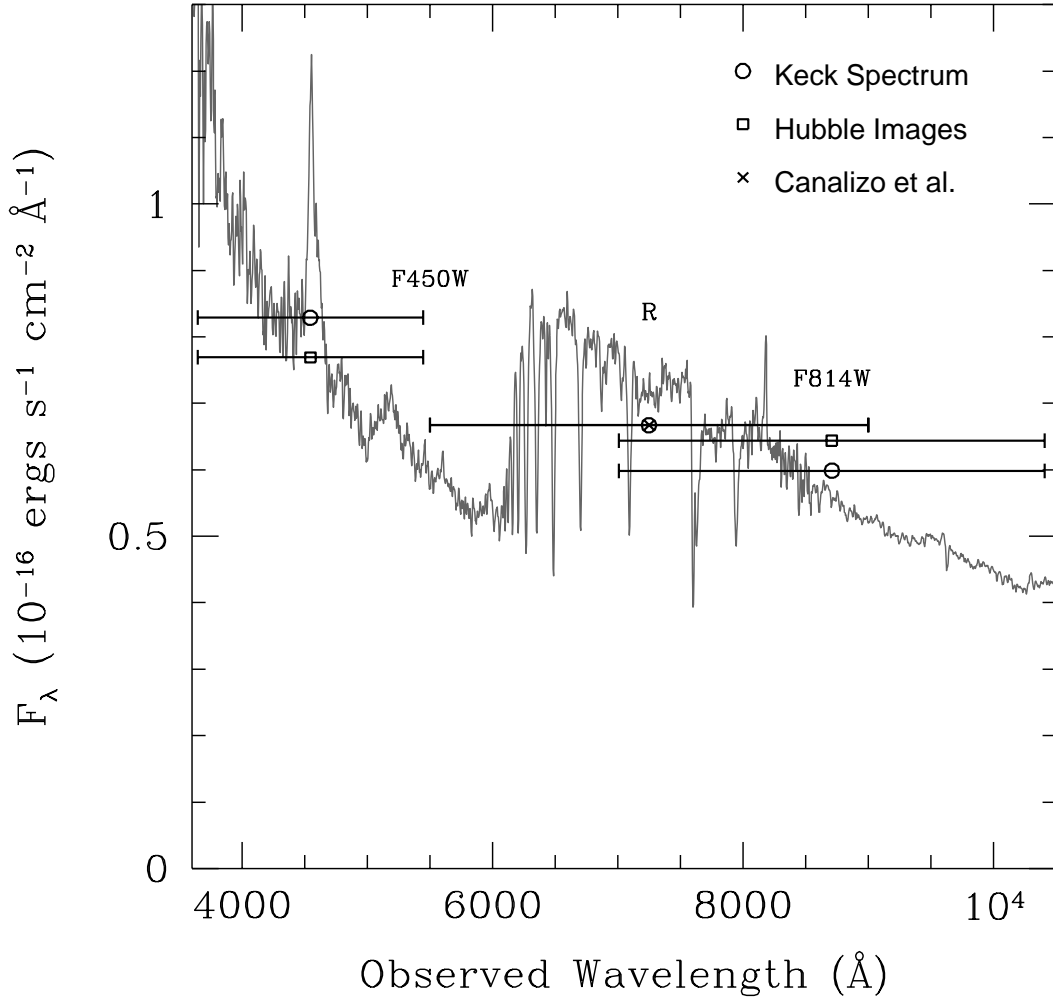


Fig. 3.— Narrow-slit Keck spectrum of UN J1025–0040 from Brotherton et al. (1999a) rescaled to match the R -band photometry of Canaliszo et al. (2000) using the IRAF task SBANDS. The F814W photometry is about 7% higher, while the F450W photometry is about 7% lower. There is no evidence for significant AGN variability.

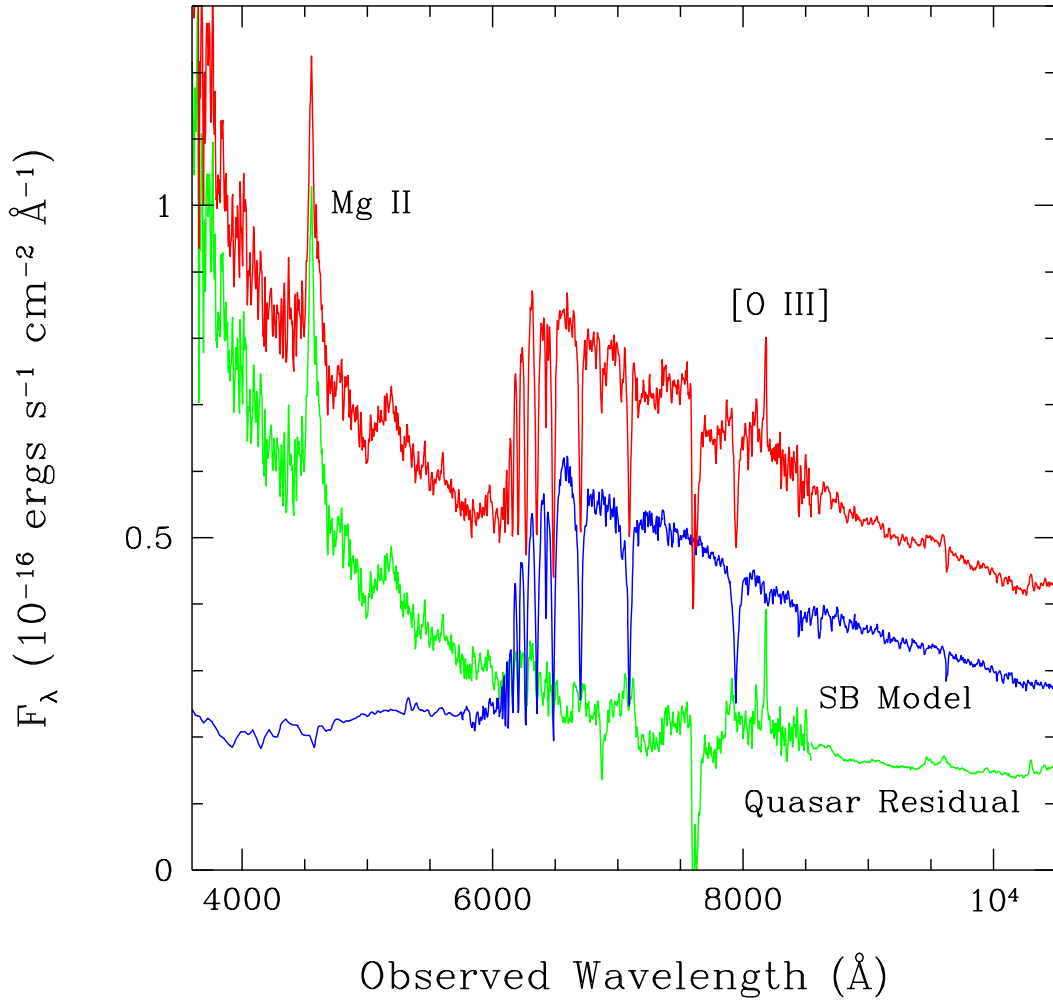


Fig. 4.— Adapted from Brotherton et al. (1999a). The top red spectrum is that of UN J1025–0040 (plus a modeled extension at long wavelengths), a 400 Myr-old instantaneous starburst (blue), and the AGN residual (green) that is the difference between the two.

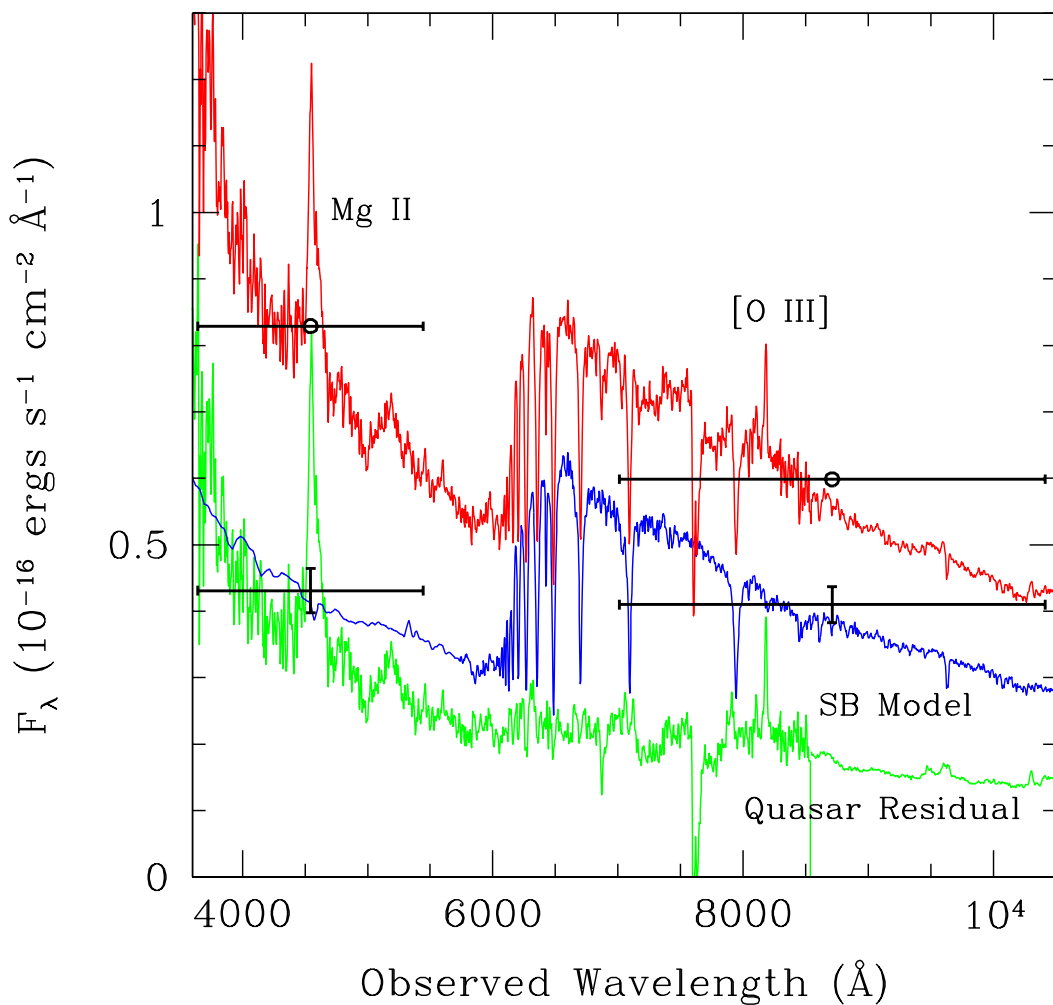


Fig. 5.— We have replotted the rescaled spectrum from Brotherton et al. (1999a) from Figure 4 (red) with the *HST*-band photometry marked (upper points) and the error bars for the non-PSF (stellar) contribution (lower points). The new starburst model (blue) is the same 400 Myr-old population as in Figure 4 plus a young population (in this case 10 Myr) and should be compared to the lower points. The quasar residual (green) is the difference between the two spectra above.

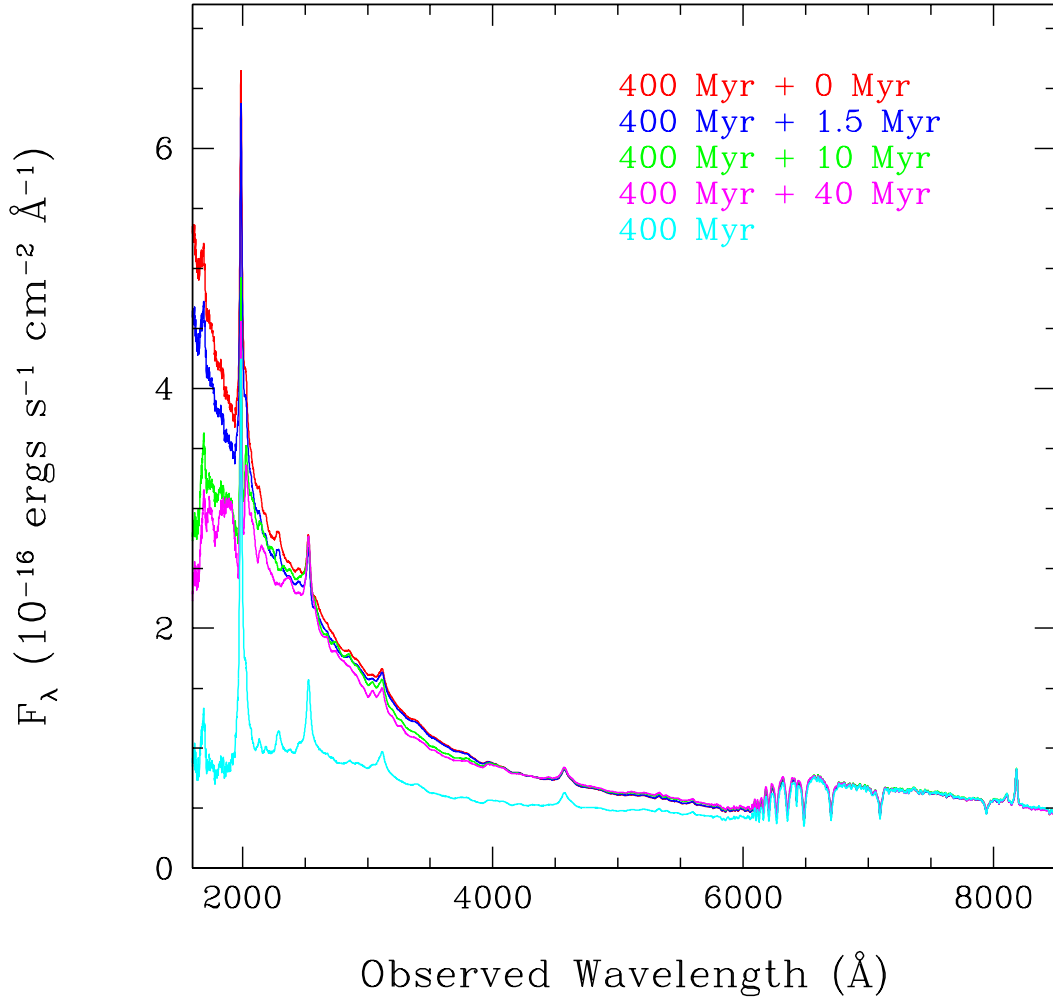


Fig. 6.— A range of viable color-coded models consisting of the composite quasar spectrum of Brotherton et al. (2001) and composite starburst models with ages indicated. The model with the 400-Myr-old population alone (light blue) does not match others since the composite quasar spectrum used has a typical power-law index and is not sufficiently blue.